Population structure promotes the evolution of costly sex in artificial gene networks

Alexander O. B. Whitlock,[1] Ricardo B. R. Azevedo,[2] iD **and Christina L. Burch[3,4]** iD

[1]*Curriculum in Genetics and Molecular Biology, University of North Carolina, Chapel Hill, North Carolina*

[2]*Department of Biology and Biochemistry, University of Houston, Houston, Texas*

[3]*Biology Department, University of North Carolina, Chapel Hill, North Carolina*

[4]*E-mail: cburch@bio.unc.edu*

We build on previous observations that Hill–Robertson interference generates an advantage of sex that, in structured populations, can be large enough to explain the evolutionary maintenance of costly sex. We employed a gene network model that explicitly incorporates interactions between genes. Mutations in the gene networks have variable effects that depend on the genetic background in which they appear. Consequently, our simulations include two costs of sex—recombination and migration loads— that were missing from previous studies of the evolution of costly sex. Our results suggest a critical role for population structure that lies in its ability to align the long- and short-term advantages of sex. We show that the addition of population structure favored the evolution of sex by disproportionately decreasing the equilibrium mean fitness of asexual populations, primarily by increasing the strength of Muller's Ratchet. Population structure also increased the ability of the short-term advantage of sex to counter the primary limit to the evolution of sex in the gene network model—recombination load. On the other hand, highly structured populations experienced migration load in the form of Dobzhansky–Muller incompatibilities, decreasing the effective rate of migration between demes and, consequently, accelerating the accumulation of drift load in the *sexual* populations.

KEY WORDS: Cost of sex, genetic architecture, Hill–Robertson interference, population structure, recombination.

Sexual reproduction—broadly defined as recombination plus outcrossing—is nearly ubiquitous among eukaryotes (Maynard Smith 1978; Bell 1982; Vrijenhoek 1998) despite its substantial costs. Foremost among these is the risk that successful, coevolved genetic interactions will be destroyed by recombination. The production of males introduces a further cost, which may approach twofold in anisogamous species (Lehtonen et al. 2012; Gibson et al. 2017). Mating can also be a costly endeavor. In many species, an individual must expend time and resources to locate a mate, risking disease and predation in the process. The widespread prevalence of sex indicates that it must convey extraordinary benefits, but the conditions that allow these benefits to counter its significant costs remain controversial.

One benefit of sex lies in its ability to increase the efficiency of natural selection by breaking up genetic associations (i.e., linkage disequilibrium) between beneficial alleles and deleterious alleles at different loci (Burt 2000; Otto and Lenormand 2002). In a phenomenon known as Hill–Robertson interference, the combined activity of selection and drift can cause genetic

associations of this kind to accumulate, such that genotypes of intermediate fitness are overrepresented in the population at the expense of genotypes of high and low fitness (Hill and Robertson 1966; Felsenstein 1974; Comeron et al. 2008). Hill–Robertson interference impairs selection even on strongly selected mutations and, in its strongest form, leads to the irreversible accumulation of drift load (Crow 1970; Poon and Otto 2000) in the form of fixed deleterious mutations, via a mechanism known as Muller's Ratchet (Muller 1964; Felsenstein 1974; Haigh 1978). Recombination decreases linkage disequilibrium, increasing the variance in fitness and restoring the efficacy of selection.

Prior theoretical work on panmictic populations demonstrated that Hill–Robertson interference, particularly in the form of Muller's Ratchet, facilitates the spread of modifiers that increase the recombination rate, that is, the *origin* of sex (Otto and Barton 2001; Iles et al. 2003; Barton and Otto 2005; Keightley and Otto 2006; Gordo and Campos 2008; Hartfield et al. 2010). However, the advantage of sex in panmictic populations was insufficient to allow the evolution of *costly* sex, except when

the modifier led to only a small increase in the probability that sex occurs (Keightley and Otto 2006; Hartfield et al. 2010). The advantage of sex was stronger in structured populations, where costly sex was able both to evolve (Martin et al. 2006) and to resist invasion by asexual mutants (Peck et al. 1999; Salathé et al. 2006; Hartfield et al. 2012).

Population structure promotes the evolution of sex by introducing two processes that have a disproportionate negative impact on asexual populations. First, population structure reduces N_e, increasing the intensity of Hill–Robertson interference (Martin et al. 2006; Hartfield et al. 2012). Second, it increases the time to fixation of invading asexual mutants, allowing more time for the operation of Hill–Robertson interference and, in particular, Muller's Ratchet (Peck et al. 1999; Salathé et al. 2006). Together, these processes have the potential to create both a long-term advantage for sexual populations, in the form of higher equilibrium mean fitness (Whitlock et al. 2016), and a short-term advantage, in the form of an increased likelihood of resisting invasion by asexual mutants (Hartfield et al. 2012). Further, the advantage of sex arising from population structure is expected to operate broadly because all natural populations show at least some structure.

The extent to which these findings can be generalized to real organisms, however, is unclear, as most of these models employed a simple genetic architecture, with limited to no interaction between genes (but see Peck et al. 1999). This precluded an important cost of sex—recombination load, which results from the disruption of coadapted gene complexes. This distinction proved vital in previous work that investigated the evolution of sex in an artificial gene network model that explicitly incorporated interactions between genes (Azevedo et al. 2006; MacCarthy and Bergman 2007; Martin and Wagner 2009; Lohaus et al. 2010; Whitlock et al. 2016). As in real biological systems, mutations in the gene networks have variable effects that depend on the genetic background in which they appear, so that both magnitude and sign epistasis (Weinreich et al. 2005) are common. In panmictic populations of artificial gene networks, the recombination load that results from sign epistasis limited the conditions under which sex was able to evolve and to be maintained, and prevented the *origin* of costly sex entirely (Whitlock et al. 2016).

Here, we evaluate the extent to which population structure supports the origin and maintenance of costly sex in the artificial gene network model, which has a complex, evolving genetic architecture (Whitlock et al. 2016). We note that the sign epistasis in the gene network model, when combined with population structure, is expected to impose another cost of sex: migration load. The offspring of sexual migrants will experience a reduction in fitness (i.e., migration load) if they carry alleles that are less compatible with alleles in resident genotypes. Migration load can therefore be understood as an extended recombination load, in which recombination between residents of different demes disrupts coadapted gene complexes and produces low-fitness hybrids. The impact of migration load on the benefits of sex imparted by population structure is unknown.

Our simulations in the artificial gene network model reveal that the relationship between population structure and the advantage of sex is non-monotonic. Small amounts of population structure did simultaneously increase both the short- and long-term advantages of sex by both disproportionately increasing the strength of Muller's Ratchet in asexual populations and delaying the time to fixation of invading asexual mutants. As a result, population structure enabled both the origin and maintenance of sex in the face of substantial costs. However, these advantages of sex were maximized in moderately structured populations. Highly structured sexual populations accumulated Dobzhansky–Muller incompatibilities that effectively prevented gene flow and, in some cases, disproportionately accelerated the accumulation of drift load (an analog of Muller's Ratchet) in *sexual* populations.

Methods

The gene network model used here is based on a model introduced by Wagner (1994, 1996).

GENOTYPE

A haploid genotype is modeled as a network of n genes, each encoding a transcription factor that can, potentially, regulate its own expression and the expression of other genes. The gene network is represented by an $n \times n$ matrix, $\mathbf{R}$, where $r_{ij} \in \mathbf{R}$ is the regulatory effect of the product of gene j on gene i. The regulatory effects are real numbers.

PHENOTYPE

The expression pattern of an individual is represented by the vector $\mathbf{S}$, where $s_i \in \mathbf{S}$ is the expression state of gene $i = 1, 2, \ldots, n$. Expression states are discrete: a gene is either on ($s_i = +1$) or off ($s_i = -1$).

The expression pattern of an individual at time τ is given by the system of recursion equations

$$s_i(\tau + 1) = f\left[\sum_{j=1}^{n} r_{ij}s_j(\tau)\right], \tag{1}$$

where f is a step function that determines how the input from the gene network controls the expression of the target gene:

$$f(x) = \begin{cases} +1 & \text{if } x \geq 0 \\ -1 & \text{otherwise} \end{cases}.$$

Starting from an initial expression pattern $\mathbf{S}(0)$ at time $\tau = 0$, gene expression changes according to equation (1) and is judged to reach a steady state if the following criterion is met:

$S(\tau) = S(\tau - 1)$. Before entering the population, genotypes undergo development. If a genotype does not achieve a gene expression steady state within $\tau \leq 100$ time steps, it is considered inviable ($W = 0$, see next section) and will not be eligible to reproduce in the subsequent generation. If a genotype achieves a gene expression steady state within $\tau \leq 100$ time steps, it is considered viable ($W > 0$), with the steady state gene expression pattern $\hat{S}$ as its *phenotype*.

FITNESS

The fitness of a viable genotype is given by

$$W = \exp\left[-\frac{\delta(\hat{S}, \dot{S})}{2\sigma^2}\right] \quad , \tag{2}$$

where $\delta(S, S') = \sum_{i=1}^{n}(s_i - s_i')^2/(4n)$ measures the difference between expression patterns S and S', $\hat{S}$ is the phenotype corresponding to the genotype, $\dot{S}$ is the optimal phenotype, and $\sigma > 0$ is inversely related to the strength of stabilizing selection.

Offspring of asexual reproduction have fitness $W_{\text{asex}} = W$, whereas offspring of sexual reproduction have fitness $W_{\text{sex}} = W/C$, where $C \geq 1$ is the cost of sex. For example, $C = 1$ and $C = 2$ represent no cost and a twofold cost, respectively.

RANDOM GENOTYPE

A random genotype is created by generating a random gene network and a random initial gene expression pattern. A random gene network is obtained by randomly filling an R matrix with $(1 - \gamma)n^2$ zeros and γn^2 random numbers from a standard normal distribution, where γ is the connectivity density of the network. γ was chosen in a manner that ensured γn^2 was an integer. A random initial gene expression pattern is generated by filling the n entries of $S(0)$ with either -1 or $+1$ with equal probability.

EVOLUTION

Evolution is simulated using an individual-based, Wright–Fisher model with non-overlapping generations. Populations maintain a constant total size, N, and are subdivided into D demes of equal size, $N_d = N/D$, arranged in a ring. In each generation, individuals undergo a selection–reproduction–mutation–migration life cycle. Structured populations consisting entirely of either sexual or asexual individuals were allowed to evolve for 10^4 generations, by which time most populations had reached an approximate mutation-recombination-selection-drift-migration fitness equilibrium (Fig. S1).

Initialization

Simulations are initiated by producing N clones of a single viable randomly generated genotype. The population's optimal phenotype is set to the phenotype of the founding individual. The optimum remains constant over the course of the simulation.

Selection

Every generation, in each deme, the N_d individuals that will reproduce are chosen at random, with replacement, with probability proportional to their fitness (eq. 2).

Reproduction

The reproductive mode of an individual is determined by its genotype at a modifier locus, *rec*, unlinked to the genes involved in the gene network. There are two alleles at the modifier locus: rec^- and rec^+. If a population is fixed for the rec^- allele, every individual reproduces asexually, and if it is fixed for the rec^+ allele, every individual reproduces sexually.

The sexual and asexual subpopulations are reproductively isolated from each other. Sexual organisms do not experience a frequency-dependent cost of finding mates. One individual is chosen for every reproductive event with probability proportional to its fitness. If it carries a rec^- allele, it reproduces asexually. If it carries a rec^+ allele, a second individual carrying a rec^+ allele is chosen with probability proportional to its fitness, and the two individuals reproduce sexually and produce one recombinant offspring. The second individual may be the same as the first individual because sampling is done with replacement, in which case the resulting reproductive event is equivalent to asexual reproduction. The recombinant R matrix is generated by copying rows from the R matrices of the parents with equal probability. This is equivalent to free recombination between regulatory regions and no recombination within regulatory regions.

Mutation

Each individual offspring acquires a random number of mutations drawn from a Poisson distribution with mean U (the genomic mutation rate). A mutation is represented by a change to the value of one of the γn^2 nonzero entries in R chosen at random; the mutated value is drawn randomly from a standard normal distribution.

Migration

Every generation, a number of individuals from each deme is randomly chosen (without replacement) to migrate to either neighboring deme, with no bias for fitness, or reproductive mode. The number of migrants from one deme to one of its neighbors is Poisson distributed with parameter $mN_d/2$, where m is the migration rate. The numbers of migrants to and from individual demes are not guaranteed to be equal. Thus, following migration the population may transiently show variation in deme sizes. Selection and reproduction restore the size of every deme to N_d.

Population structure

We manipulated population structure in two ways. First, we investigated populations subdivided into equally sized demes, producing deme sizes (N_d) of 10, 12, 15, 20, 33, 50, 67, 83, or 100 individuals. Demes were arranged around a circle and migration occurred via a one-dimensional stepping-stone model (Kimura 1952). Second, we varied the migration rate (m) between neighboring demes, using rates equal to 2×10^{-4}, 2×10^{-3}, 2×10^{-2}, or 0.2. There was no migration (i.e., $m = 0$) between non-neighboring demes.

INVASION ANALYSES

Populations were evolved for 10^4 generations under asexual (or sexual) reproduction to allow sufficient time for the population to approach mutation–recombination–selection–drift–migration fitness equilibrium. We then mutated the allele at the modifier locus rec ($rec^- \leftrightarrow rec^+$, see "Reproduction" above) in a single randomly chosen individual, causing it to switch to the opposite reproductive mode, from asexual to sexual or vice versa. We measured the fixation probability of the novel modifier allele, u, relative to that of a neutral mutation ($u^* = 1/N$) in replicate invasion trials. During the invasion trials, individuals carrying the sexual modifier allele rec^+ experience a fixed cost of sex, C (see "Fitness" above). For invasion trials in which the novel modifier allele fixed, we recorded the generation in which it fixed as T_{fix}. For each combination of N_d, m, and C that we examined, we conducted 50 replicate invasion trials for each of 50 founders, for a total of 2500 replicate trials.

EVOLUTION OF RECOMBINATION RATE

Populations were evolved for 10^4 generations with a modifier locus that was linked to a randomly chosen element of the **R** matrix and fixed for an allele that specified a map length of $\lambda = 0$ M. After generation 10^4, the modifier locus experienced mutations at a rate of 10^{-3} per generation. Mutational effects on λ were ± 0.05 M, with equal probability. Mutations that conferred $\lambda < 0$ were discarded. When two individuals with map lengths λ_1 and λ_2 reproduced, the expected number of crossovers in the offspring was $\lambda_1 + \lambda_2$. Crossover locations were chosen randomly and occurred between elements of the **R** matrix.

POPULATION METRICS

Mean fitness. We define $\overline{W}$ as the mean fitness of all individuals present in the population at a given time (see eq. 2). The mean fitness of sexual and asexual individuals is denoted by $\overline{W}_{\text{sex}}$ and $\overline{W}_{\text{asex}}$, respectively.

Rate of adaptation. We define the rate of adaptation as

$$v = \frac{\ln \overline{W}_2 - \ln \overline{W}_1}{\ln t_2 - \ln t_1}, \quad (3)$$

where $\overline{W}_i$ is mean fitness at generation t_i of the initial evolution experiment. We used $t_1 = 562$ and $t_2 = 1778$ generations in our calculations because a visual inspection of the fitness trajectory data (Fig. S1) indicates that drift load accumulated over this time interval under a wide range of parameters. The results of all statistical analyses that included this rate of adaptation metric were qualitatively and quantitatively robust to both the location and length of this time interval, as long as $t_1 \gtrsim 100$ generations.

Deleterious mutation rate

We define the deleterious mutation rate as $U_d = U(p_l + p_d)$, where U is the genomic mutation rate, and p_l and p_d are the proportions of lethal and nonlethal deleterious mutations, respectively. U is constant throughout the course of a simulation but p_l and p_d can evolve. We estimated the quantity $p_l + p_d$ for a genotype by generating 100 mutant copies of the genotype, each carrying one independently generated mutation, and evaluating the proportion of them that have lower fitness than the original genotype.

Epistasis

We define multiplicative epistasis between two nonlethal mutations, i and j, as $\varepsilon = W_{ij}/W - W_i W_j / W^2$, where W is the fitness of the unmutated genotype, W_i and W_j are the fitnesses of the single mutants, and W_{ij} is the fitness of the double mutant. We calculated mean epistasis coefficients, ε, across a random sample of 100 pairs of mutations, introduced individually and in combination into each viable individual in the population.

Mean fitness of recombinant offspring

We define the mean fitness of recombinant offspring, $\overline{W}_R$, as the mean fitness of offspring produced by recombination (without mutation) between sexually reproducing individuals of the same deme, W_r, relative to the average fitness of its parents $\overline{W}_p$. We averaged $W_r/\overline{W}_p$ across N independently chosen pairs of individuals, where each parent was chosen with probability proportional to its fitness (i.e., in the same way the population reproduced in the evolutionary simulations).

Mean fitness of migrant offspring

We define the mean fitness of migrant offspring, $\overline{W}_M$, as the mean fitness of offspring produced by recombination (without mutation) between sexually reproducing individuals of neighboring demes, W_m, relative to the average fitness of its parents $\overline{W}_p$. We averaged $W_m/\overline{W}_p$ across N independent offspring, generated by recombination between N_d pairs of parents randomly chosen from each of the D pairs of neighboring demes. Both parents were chosen from among the individuals in their respective demes with probability proportional to their fitness.

Population differentiation

We quantify genetic differentiation between populations as $F_{ST} = V_b/(V_w + V_b)$, where V_w and V_b are the variance within and among demes at a neutral locus, respectively. Each individual carries 20 neutral loci, which were neither linked to each other nor to any of the gene network loci. The founding genotype had a value of 0 at all 20 neutral loci. Every generation, each neutral locus in each individual acquired a random number of mutations drawn from a Poisson distribution with mean 1.0 (the neutral locus mutation rate). Each mutation changed the value of the neutral locus by adding a random value drawn from the standard normal distribution. V_w and V_b were calculated as variance components of the numerical values at each neutral locus in a random-effects analysis of variance. We calculated F_{ST} for each of the 20 neutral loci and report the average of these values.

Maximum cost of sex

We described the maximum sustainable cost of sex during the origin and maintenance of sex as origin-C_{max} and maintenance-C_{max}, respectively. Origin-C_{max} is the maximum value of C for which $u_{sex} > u^*$ in sexual invasion trials. Maintenance-C_{max} is the maximum value of C for which $u_{asex} < u^*$ in asexual invasion trials (see "Invasion analyses"). For each set of equilibrium populations evolved at a particular m and N_d, we measured the modifier fixation probability, u, at each of at least four values of C and estimated C_{max} from the resulting data using logistic regression (Figs. S2 and S3).

Equilibrium values

The equilibrium values are defined as values of population metrics at generation 10^4 (Fig. S1) and indicated by a hat symbol (e.g., $\hat{\bar{W}}_{sex}$).

PARAMETER VALUES

We used the same parameters as in Whitlock et al. (2016): networks of $n = 100$ genes with connectivity density $\gamma = 0.05$, a genomic mutation rate of $U = 1$ per generation, and stabilizing selection ($\sigma^2 = 0.1$). Using these parameters, mutations have a broad range of potential fitness effects, including beneficial, neutral, slightly deleterious, and lethal (Fig. S4). Random genotypes have a deleterious mutation rate of $U_d \approx 0.5$ (Fig. S5; Fig. S1 of Whitlock et al. 2016). This value is comparable to those estimated for fruit flies ($U_d = 0.6$, Haag-Liautard et al. 2007) and rodents ($U_d = 0.5$, Gaffney and Keightley 2006).

We simulate populations of $N = 10^3$ individuals. We chose this value because it is the largest population size in which sex is approximately neutral in the short term in panmictic populations (see Fig. 4 of Whitlock et al. 2016), so that any advantage or disadvantage to sex observed here in either sexual or asexual invasion trials can be attributed to population structure. Our choice

not to vary the overall population size, N, also focused our attention on differences in the accumulation of drift, recombination, and migration loads that were driven by differences in N_d and m, rather than differences in N.

STATISTICAL ANALYSIS

All statistics were conducted using the R statistical package, version 3.4.1 (Ihaka and Gentleman 1996). Logistic regression was conducted using the function *glm* from the *stats* package. Linear models that investigated the contributions of various population metrics to the long- and short-term advantages of sex were conducted using the function *lm* from the *stats* package.

All data were generated from 50 pairs of sexual and asexual populations. Each pair was founded by an independent, randomly generated genotype. Combined metrics from sexual and asexual populations, like $\hat{\bar{W}}_{sex}/\hat{\bar{W}}_{asex}$, were calculated separately for each pair, and the resulting 50 composite values were used for plotting and statistical tests.

Results
POPULATION STRUCTURE HAS A COMPLEX EFFECT ON THE LONG-TERM ADVANTAGE OF SEX

Previously, it was shown that panmictic (i.e., unstructured) sexual populations of $N = 10^3$ individuals experiencing a genomic mutation rate of $U = 1$ and moderate stabilizing selection ($\sigma^2 = 0.1$) evolved a mean fitness at equilibrium $5.7 \pm 0.8\%$ (mean and 95% confidence interval) higher than that of otherwise identical asexual populations (Whitlock et al. 2016). Here we investigate the extent to which population structure increases the long-term advantage of sex.

The least structured populations (i.e., those subdivided into $D = 10$ demes of $N_d = 100$ individuals each, experiencing the highest migration rate, $m = 0.2$) evolved approximately like panmictic populations, achieving similar equilibrium mean fitness and $F_{ST} \approx 0$ (Figure 1). Decreasing either the deme size (N_d) or the migration rate (m) caused the level of genetic differentiation among demes, F_{ST}, to increase, confirming that populations became more structured (Fig. 1).

Relative to panmictic populations, small increases in population structure, imposed by decreasing either N_d or m, caused the magnitude of the long-term advantage of sex ($\hat{\bar{W}}_{sex}/\hat{\bar{W}}_{asex}$) to increase (Fig. 1). This pattern was true provided the population consisted of relatively large demes ($N_d \gtrsim 50$). At $N_d = 50$ and $m = 2 \times 10^{-4}$, the average advantage of sex achieved a maximum that was 5.8-fold larger than it was in a panmictic population of the same total size.

Indeed, for each $m \leq 2 \times 10^{-2}$, there was an intermediate deme size, N_d^*, at which the advantage of sex was maximized. Further subdivision into demes that were smaller than
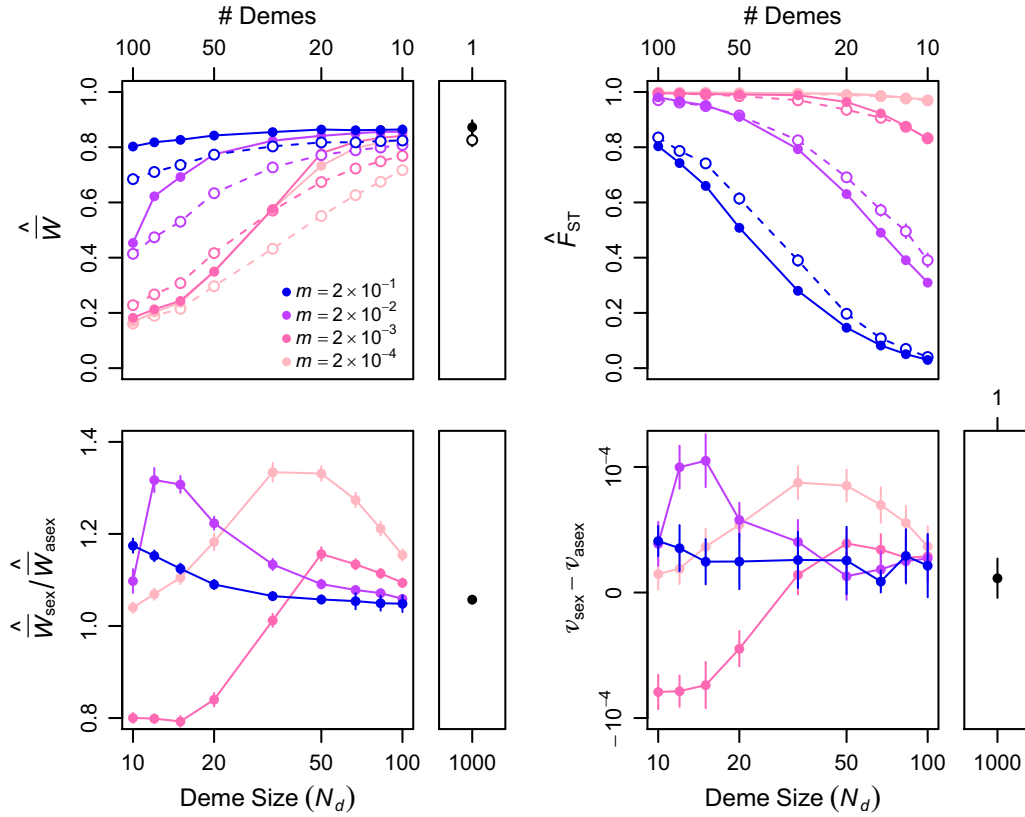
Figure 1. Migration rate and population subdivision interact in a complex way to determine the long-term advantage of sex. Mean fitness ($\bar{\hat{W}}$), the fitness advantage of sexuals ($\bar{\hat{W}}_{\text{sex}}/\bar{\hat{W}}_{\text{asex}}$), and population differentiation ($\hat{Q}_{ST}$) were calculated at generation 10^4, after populations of all migration rates and deme sizes had achieved approximate fitness equilibria. The rate of adaptation of sexual populations relative to that of asexual populations ($v_{\text{sex}} - v_{\text{asex}}$) was calculated using data from generations 562 and 1778 (see eq. 3). In the top panels, sexual and asexual populations are represented by closed and open circles, respectively. Large panels show the relationships between these equilibrium metrics and the deme number and size of subdivided populations. Small panels show the equilibrium metrics calculated from panmictic asexual and sexual populations of the same total size, $N = 10^3$ (obtained as in Whitlock et al. 2016). Values are means and 95% confidence intervals based on 50 replicate populations initiated from different randomly chosen founders.

N_d^* eroded the advantage of sex. Surprisingly, the effect of small deme size was most pronounced at the intermediate migration rate of $m = 2 \times 10^{-3}$, such that the only conditions in which sex was disadvantageous were observed in the smallest deme sizes ($N_d \leq 20$) at this migration rate.

The variance we observed in the long-term advantage of sex was almost entirely explained by the rate of adaptation (see eq. 3) in sexual (v_{sex}) relative to asexual (v_{asex}) populations (linear regression of $\bar{\hat{W}}_{\text{sex}}/\bar{\hat{W}}_{\text{asex}}$ against $v_{\text{sex}} - v_{\text{asex}}$: $R^2 = 0.95$, $F_{1,34} = 669.3$, $P < 10^{-15}$; Fig. 1). We note that v is a composite metric that increases with adaptation rate and decreases with the accumulation of genetic load. Although v, by definition, measures the rate of adaptation, in our simulations differences in v may better reflect differences in the rate of accumulation of genetic load—specifically drift load in the form of fixed deleterious mutations. $v_{\text{sex}} - v_{\text{asex}}$ took on its highest values for combinations of m and N_d in which migration effectively reduced the

accumulation of drift load in sexual ($v_{\text{sex}} > 0$) but not asexual ($v_{\text{asex}} < 0$) populations. In these conditions, asexual populations experienced Muller's Ratchet. Conditions in which drift load accumulated in both sexuals and asexuals, but did so more rapidly in sexuals ($v_{\text{sex}} < v_{\text{asex}} < 0$), were observed despite being entirely unexpected. We next investigated the cause of the accelerated accumulation of drift load in some of the highly structured sexual populations.

DOBZHANSKY–MULLER INCOMPATIBILITIES ACCELERATE THE ACCUMULATION OF DRIFT LOAD IN STRUCTURED SEXUAL POPULATIONS

We hypothesized that evolving properties of the genetic architecture made substantial contributions to the rate at which drift load accumulated. Thus, we measured the mutation, recombination, and migration loads of equilibrium structured populations. Both the mutation and recombination loads evolved

in ways that contributed to differences among treatments in equilibrium mean fitness (Fig. 2), as was observed previously in panmictic populations (Whitlock et al. 2016). The lower equilibrium $\hat{\bar{U}}_d$ of sexual, compared to asexual, populations generated a fitness advantage for sexual populations of 6–9% ($1.06 < \exp(-\hat{\bar{U}}_{d,\text{sex}})/\exp(-\hat{\bar{U}}_{d,\text{asex}}) < 1.09$). Recombination load at equilibrium generated a fitness *disadvantage* for sexual populations of 5–8% ($0.92 < \hat{\bar{W}}_R < 0.95$). However, the differences among treatments in mutation and recombination loads (Fig. 2) cannot explain the differences among treatments in the overall advantage to sex (Fig. 1; linear regression of $\hat{\bar{W}}_{\text{sex}}/\hat{\bar{W}}_{\text{asex}}$ against $\exp(-\hat{\bar{U}}_{d,\text{sex}})/\exp(-\hat{\bar{U}}_{d,\text{asex}})$: $R^2 = 0.0937$, $F_{1,34} = 3.514$, $P = 0.0695$; linear regression against $\hat{\bar{W}}_R$: $R^2 = 0.0153$, $F_{1,34} = 0.5275$, $P = 0.4726$).

A third property of the genetic architecture, the relative fitness of sexual migrant offspring, $\overline{W}_M$, also evolved in our simulations (Fig. 2). At equilibrium, $\hat{\overline{W}}_M$ depended predictably on both N_d and m. For large N_d and m, the fitness of migrant offspring was indistinguishable from that of resident offspring (i.e., $\overline{W}_M \approx \overline{W}_R$), as expected when there is relatively little differentiation between demes (low $\hat{F}_{ST}$). As N_d and m declined, so did $\hat{\overline{W}}_M$, until when $N_d \lesssim 50$ and $m \leq 2 \times 10^{-3}$, demes were strongly differentiated (high $\hat{F}_{ST}$) and $\hat{\overline{W}}_M \approx 0$. These reductions in $\hat{\overline{W}}_M$ must have resulted from the accumulation of alleles in some demes that show strong negative epistatic interactions with alleles present in other demes—that is, Dobzhansky–Muller incompatibilities. This extreme variation in $\hat{\overline{W}}_M$ had only a negligible direct effect on population mean fitness because $\hat{\overline{W}}_M$ was low only when migration rates were also low ($m \lesssim 2 \times 10^{-3}$). Instead, the main consequence of a low $\hat{\overline{W}}_M$ was to reduce the effective gene flow between demes, which in turn intensified the accumulation of drift load in sexual populations.

In highly structured populations with moderate migration rates (e.g., $N_d < 33$ and $m = 2 \times 10^{-3}$; Fig. S1; Fig. 2, dark pink), the accumulation of Dobzhansky–Muller incompatibilities ($\overline{W}_M \approx 0$) explains the faster fitness declines in sexual than in asexual populations ($v_{\text{sex}} < v_{\text{asex}}$; hot pink line in Fig. 1). In this parameter range, the moderate migration experienced only by asexual populations more effectively countered Muller's Ratchet than the recombination experienced only by sexual populations. Outside this parameter range, the effective migration rate was similar in asexual and sexual populations, either because Dobzhansky–Muller incompatibilities did not accumulate in sexual populations ($m > 10^{-3}$) or because the migration rate was also near zero in asexual populations ($m = 10^{-4}$).

These results depended quantitatively, but not qualitatively, on the relatively high network connectivity ($\gamma = 0.05$) and mutation rate ($U = 1$) we employed in these simulations. Qualitatively, the dependency of the long-term advantage of sex on the relative rate of adaptation in sexuals ($v_{\text{sex}} - v_{\text{asex}}$) remains strong at both
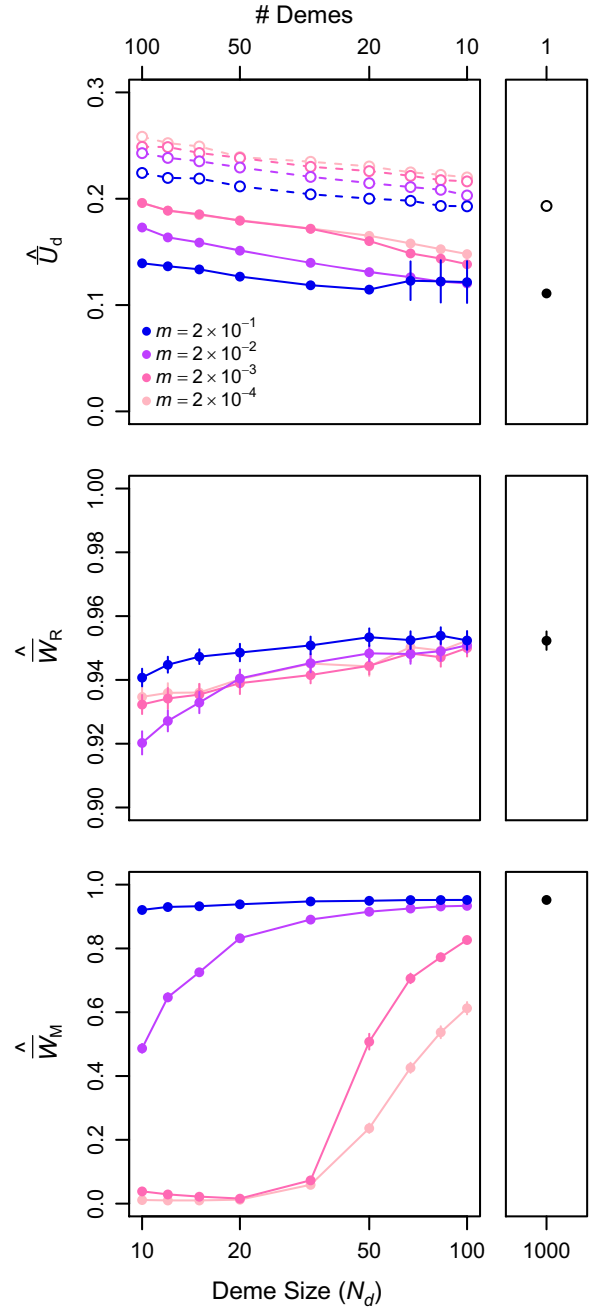

Figure 2. Migration rate and deme size affect three aspects of the equilibrium genetic architecture. Deleterious mutation rate ($\hat{\bar{U}}_d$), the mean fitness of recombinant offspring of parents from the same deme ($\hat{\overline{W}}_R$), and the mean fitness of recombinant offspring of parents from different demes ($\hat{\overline{W}}_M$) at generation 10^4, after populations of all migration rates and deme sizes achieved approximate fitness equilibria. Large panels show the relationships between these equilibrium metrics and the deme number and size of subdivided populations. Small panels show the equilibrium metrics calculated from panmictic asexual and sexual populations of size $N = 10^3$ (obtained as in Whitlock et al. 2016). During the evolution experiments, offspring produced by asexual reproduction experience $W_R = 1$ and $W_M = 1$, by definition. Symbols and error bars as described in Figure 1.
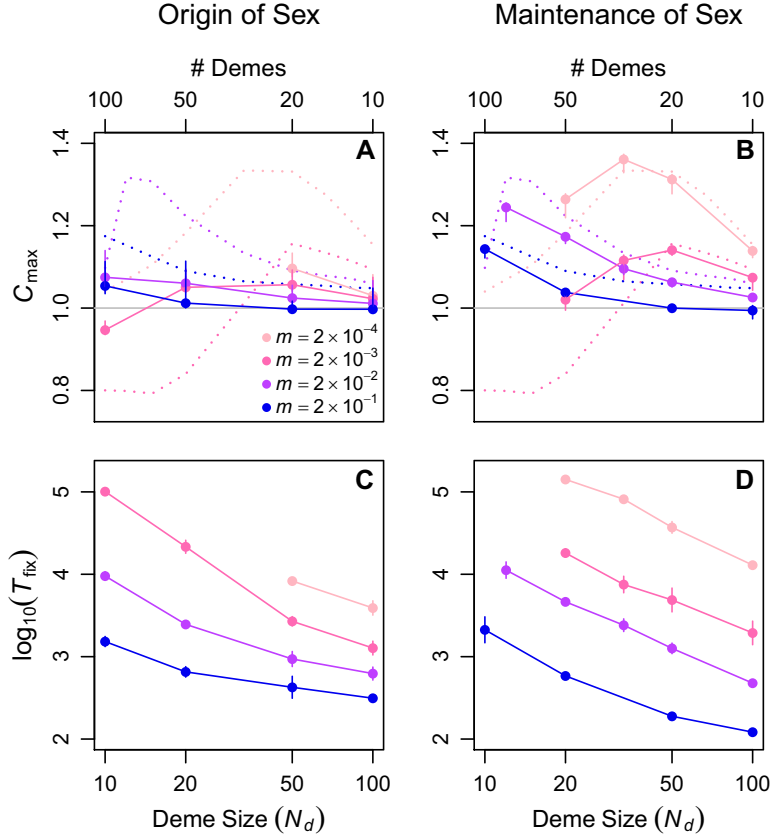
Figure 3. Population structure increases the transit time (T_{fix}) of invading sexual and asexual mutants, facilitating both the origin and maintenance of costly sex. (A) Points connected by solid lines show the maximum cost of sex at which sexual mutants successfully invaded equilibrium asexual populations in each deme size and migration rate treatment (origin-C_{max}). (B) Points connected by solid lines show the maximum cost of sex at which equilibrium sexual populations successfully resisted invasion by asexual mutants (maintenance-C_{max}). Dotted lines in both (A) and (B) show the long-term advantage of sex, $\hat{W}_{\text{sex}}/\hat{W}_{\text{asex}}$, replotted from Figure 1, for comparison. (C and D) The average fixation time (T_{fix}) of sexual (C) and asexual (D) mutants that successfully invaded equilibrium asexual and sexual populations, respectively. Values are means and 95% confidence intervals based on all of the successful invasions in each condition. Missing points in the $m = 2 \times 10^{-3}$ and $m = 2 \times 10^{-4}$ series correspond to parameter combinations for which invasion trials were not run because they were not computationally feasible (i.e., T_{fix} was too long).

lower connectivity ($\gamma = 0.02$; Fig. S6) and lower mutation rate ($U = 0.1$; Fig. S7). Quantitatively, reducing network connectivity reduced the extent to which mutational (Fig. S6, $p_d + p_l$) and epistatic effects (Fig. S6, $\hat{W}_R$ and $\hat{W}_M$) could evolve, resulting in a smaller disadvantage of sex in the more structured populations (Fig. S6, $m \lesssim 2 \times 10^{-3}$), but affecting the advantage of sex in the less structured populations very little (Fig. S6, $m \gtrsim 2 \times 10^{-2}$). Reducing the mutation rate reduced the strength of drift load, resulting in both a smaller advantage of sex in the less structured populations (Fig. S7, $m \gtrsim 2 \times 10^{-2}$) and a larger disadvantage of sex in the more structured populations (Fig. S7, $m \lesssim 2 \times 10^{-3}$).

THE RELATIVE RATE OF ADAPTATION IS ALSO A GOOD PREDICTOR OF THE EVOLUTIONARY SUCCESS OF SEX

Previously, it was shown in the artificial gene network model that sex could neither evolve nor be maintained in panmictic popula-

tions of $N = 10^3$. At this population size, newly arising sexual and asexual modifier mutations were both statistically indistinguishable from neutral mutations in their probability of invading equilibrium populations of the other reproductive mode (Whitlock et al. 2016). Here, we investigate the extent to which the predicted effects of population structure on differences in the rate at which drift load accumulates, $v_{\text{sex}} - v_{\text{asex}}$, and on the time, T_{fix}, that modifier mutations spend in transit to fixation combine to promote the origin and maintenance of costly sex.

As expected, population structure promoted the maintenance of costly sex (Fig. 3B, D). For each combination of m and N_d, we used invasion assays to estimate the maximum cost of sex (maintenance-C_{max}) under which the fixation probability of an asexual modifier mutation was lower than the neutral expectation ($u < u^*$, Fig. S2). Maintenance-$C_{\text{max}} > 1$ for almost all the parameter combinations, we examined and rose as high as 1.36 for the most favorable parameter combination.
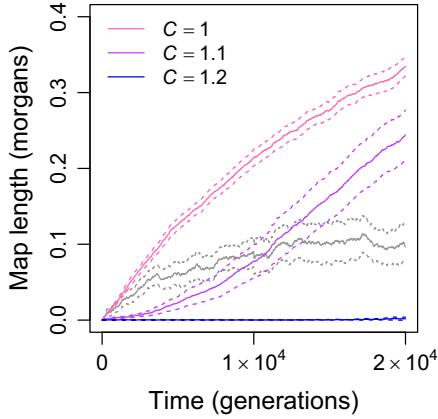
Figure 4. Evolution of the recombination rate under recurrent mutation at the recombination modifier locus. Solid and dashed color lines show the change in mean and 95% confidence interval, respectively, of the genome map length (i.e., mean crossover probability) over time in structured populations with $N_d = 50$ and $m = 2 \times 10^{-4}$ and costs of sex ranging from none ($C = 1$, pink) to substantial (purple and blue). Panmictic populations of the same total size ($N = 10^3$) experiencing no cost of sex ($C = 1$) are shown in gray for comparison. Data are from 50 replicates initiated with the equilibrium structured asexual populations shown in Figures 1 and S1 (pink, purple, and blue) or the equilibrium panmictic asexual populations of size $N = 10^3$ (gray, as in Whitlock et al. 2016).

Maintenance-C_{max} significantly increased with both $v_{sex} - v_{asex}$ (regression against $v_{sex} - v_{asex}$: $F_{1,14} = 279.1$, $P < 10^{-9}$) and the mean T_{fix} among successful invaders (regression of maintenance-C_{max} against $\log_{10} T_{fix}$: $F_{1,14} = 135.6$, $P < 10^{-7}$). Indeed, $v_{sex} - v_{asex}$ and T_{fix} predicted maintenance-C_{max} almost perfectly (multiple regression model with both predictors: $R^2 = 0.97$; compared to the model with only $v_{sex} - v_{asex}$: $R^2 = 0.65$).

Population structure also promoted the origin of costly sex (Fig. 3A, C). To investigate the origin of sex, we used invasion assays to estimate the maximum cost of sex (origin-C_{max}) under which the fixation probability of a sexual modifier mutation was higher than the neutral expectation ($u > u^*$, Fig. S3). Similar to maintenance-C_{max}, origin-$C_{max} > 1$ for almost all the parameter combinations we examined and increased significantly with both $v_{sex} - v_{asex}$ (regression against $v_{sex} - v_{asex}$: $F_{1,11} = 17.24$, $P = 0.0016$) and T_{fix} (regression against T_{fix}: $F_{1,11} = 8.28$, $P = 0.0150$). However, origin-C_{max} rose only as high as 1.1 for the most favorable parameter combination and was only somewhat predictable from the quantities T_{fix} and $v_{sex} - v_{asex}$ (multiple regression model with both predictors: $R^2 = 0.70$).

We note that these results are for modifiers of sex that cause free recombination between rows of the genotype matrix, **R**. We also examined the behavior of modifiers of recombination that cause only small changes in recombination rate, using a model that allows recurrent mutation at the modifier locus. Modifiers of recombination behaved similarly to modifiers of sex. Using the parameter combination that was most favorable to the origin of sex, recombination rate increased over time when $C = 1.1$, but not when $C = 1.2$ (Fig. 4). This similarity between the two types of modifiers was not observed in panmictic populations, where modifiers of recombination were more likely to evolve than modifiers of sex (Whitlock et al. 2016).

Discussion

Our work builds on prior observations that Hill–Robertson interference generates an advantage of sex that, in structured populations, can be large enough to explain the evolutionary maintenance of *costly* sex (Peck et al. 1999; Martin et al. 2006; Salathé et al. 2006; Hartfield et al. 2012). By investigating the evolution of sex using an artificial gene network model, our simulations differed from the prior work by including the type of genetic interaction (sign epistasis, Weinreich et al. 2005) that results in recombination load and migration load. Some of our results did not depend on this difference. For instance, population structure had the expected effect of disproportionately increasing the strength of Muller's Ratchet in asexual lineages, facilitating both the origin and the maintenance of sex. Other results depended critically on the abundant sign epistasis in the gene network model. In particular, highly structured populations experienced migration load in the form of Dobzhansky–Muller incompatibilities that accelerated the accumulation of drift load in sexual populations and reduced the long-term advantage of sex.

To our knowledge, our first observation, that population structure promoted the origin of sex, has not been investigated previously by either theory or simulation. Our results indicate that the effect of population structure on the origin of sex resulted primarily from a structure-driven reduction in the rate at which drift load accumulated in sexual compared to asexual lineages (measured as $v_{sex} - v_{asex}$). The smaller but significant effect of T_{fix} on origin-C_{max} suggests that structure not only slowed the fixation of sexual invaders, it also slowed their loss during the first several hundred generations, before recombination load had been ameliorated by the evolution of recombinational robustness. If our interpretation of the relationship between T_{fix} and origin-C_{max} is correct, it suggests that structure ameliorates the barrier to the origin of sex posed by recombination load.

Our second observation, that the long-term advantage of sex was maximized at intermediate structure, was not predictable from prior work conducted using simpler genetic architectures (that lacked sign epistasis). As in the prior work, we confirmed that the long-term advantage of sex in the gene-network model depended on differences in the rate at which drift load accumulated in sexual and asexual populations. These differences

depended, in turn, on the effective rate of migration between demes, $m_e \approx m \overline{W}_M$. In the gene-network model, increasing structure promoted the accumulation of Dobzhansky–Muller incompatibilities in sexual populations (Dobzhansky 1937; Muller 1942; Bank et al. 2012), which in turn decreased the effective migration rate. In the most structured sexual populations, the mean fitness of hybrids between demes dropped to $\overline{W}_M \approx 0$ and the effective migration rate dropped to $m_e \approx 0$. Asexual populations did not experience migration load (i.e., $\overline{W}_M = 1$ and $m_e = m$) because asexual migrant alleles did not change genetic backgrounds and were equally well adapted to local and distant environments. Thus, asexual populations benefited from migration in some high-structure conditions (e.g., $m = 10^{-3}$ and $N_d < 33$) where sexual populations did not. In these conditions, drift load accumulated faster in sexual than in asexual populations. Strong Dobzhansky–Muller genetic incompatibilities have been observed in other computational models (e.g., a model very similar to ours: Palmer and Feldman 2009; models of transcription-factor binding: Tulchinsky et al. 2014, Khatri and Goldstein 2015; a model of RNA folding: Kalirad and Azevedo 2017), as well as within (Cutter 2012; Corbett-Detig et al. 2013) and among (Presgraves 2010; Maheshwari and Barbash 2011) biological species in nature. In addition, Dobzhansky–Muller incompatibilities between populations have been observed to evolve in as few as 500 generations in the laboratory (Anderson et al. 2010). Thus, their evolution over the course of 10^4 generations in our simulations was not unexpected.

Earlier work has shown that migration load could generate a cost of sex in structured populations experiencing spatially *heterogeneous* selection (García-Ramos and Kirkpatrick 1997; Kirkpatrick and Barton 1997; Hendry et al. 2001; Alleaume-Benharira et al. 2006; Bolnick and Nosil 2007). Our results extend the potential role of migration load as a cost of sex to structured populations under spatially *homogeneous* selection. Our data also revealed a general mechanism for the cost of sex caused by migration load. Migration load, whether generated by the accumulation of Dobzhansky–Muller incompatibilities or by local maladaptation, reduces the effective migration rate, which intensifies the accumulation of drift load in sexual populations.

The advantages and disadvantages of sex that we observed here depended critically on the magnitudes of drift, mutation, recombination, and migration loads, and the extent to which these loads were evolvable properties of the populations of gene networks. In turn, these sources of genetic load depended not only on the population structure parameters N_d and m, but also on the genetic parameters U and γ. Reducing the mutation rate had the expected effect of reducing both mutation and drift loads in asexual populations, so that even the most favorable population structure conditions yielded only very small fitness advantages to sexual populations. Also as expected, the strongest effects of net-

work connectivity were on the magnitudes of recombination and migration loads. In that case, decreasing γ had only small effects in conditions in which sex experienced an overall advantage (resulting from reduced drift load), but had relatively strong effects in conditions in which sex experienced an overall disadvantage (resulting from increased migration load).

In sum, our results demonstrate that complex genetic architecture can interact with population structure to either promote or constrain the origin and maintenance of costly sex. In our simulations, sex was maintained in the face of costs as high as $C = 1.36$, but not as high as twofold. However, the magnitude of both the long- and short-term advantages of sex are likely to be affected by many factors not considered here, including the pattern of migration between demes, deviations from random mating other than those arising from population structure, coevolutionary interactions, ploidy, and environmental change (Shields 1982; Kirkpatrick and Jenkins 1989; Kondrashov and Crow 1991; Charlesworth 1993; Ladle et al. 1993; Barton 1995; Judson 1997; Agrawal 2001; Agrawal and Chasnov 2001; Siller 2001; Otto 2003; Otto and Nuismer 2004; Blachford and Agrawal 2006; Combadão et al. 2007; Carja et al. 2014; Nowak et al. 2014). We posit that these factors may also interact with a complex genetic architecture to influence the evolution of sex, making them promising avenues for future inquiry.

LITERATURE CITED

Agrawal, A. F. 2001. Sexual selection and the maintenance of sexual reproduction. Nature 411:692–695.

Agrawal, A. F., and J. R. Chasnov. 2001. Recessive mutations and the maintenance of sex in structured populations. Genetics 158:913–917.

Alleaume-Benharira, M., I. R. Pen, and O. Ronce. 2006. Geographical patterns of adaptation within a species' range: interactions between drift and gene flow. J. Evol. Biol. 19:203–215.

Anderson, J. B., J. Funt, D. A. Thompson, S. Prabhu, A. Socha, C. Sirjusingh, J. R. Dettman, L. Parreiras, D. S. Guttman, A. Regev, and L. M. Kohn. 2010. Determinants of divergent adaptation and Dobzhansky-Muller interaction in experimental yeast populations. Curr. Biol. 20:1383–1388.

Azevedo, R. B. R., R. Lohaus, S. Srinivasan, K. K. Dang, and C. L. Burch. 2006. Sexual reproduction selects for robustness and negative epistasis in artificial gene networks. Nature 440:87–90.

Bank, C., R. Bürger, and J. Hermisson. 2012. The limits to parapatric speciation: Dobzhansky–Muller incompatibilities in a continent–island model. Genetics 191:845–863.

Barton, N. H. 1995. A general model for the evolution of recombination. Genet. Res. 65:123–145.

Barton, N. H., and S. P. Otto. 2005. Evolution of recombination due to random drift. Genetics 169:2353–2370.

Bell, G. 1982. The Masterpiece of Nature: The Evolution and Genetics of Sexuality. Univ. of California Press, Berkeley.

Blachford, A., and A. F. Agrawal. 2006. Assortative mating for fitness and the evolution of recombination. Evolution 60:1337–1343.

Bolnick, D. I., and P. Nosil. 2007. Natural selection in populations subject to a migration load. Evolution 61:2229–2243.

Burt, A. 2000. Perspective: Sex, recombination, and the efficacy of selection— Was Weismann right? Evolution 54:337–351.

Carja, O., U. Liberman, and M. W. Feldman. 2014. Evolution in changing environments: Modifiers of mutation, recombination, and migration. Proc. Natl. Acad. Sci. USA 111:17935–17940.

Charlesworth, B. 1993. Directional selection and the evolution of sex and recombination. Genet. Res. 61:205–224.

Combadão, J., P. R. A. Campos, F. Dionisio, and I. Gordo. 2007. Small-world networks decrease the speed of Muller's ratchet. Genet. Res. 89: 7–18.

Comeron, J. M., A. Williford, and R. M. Kliman. 2008. The Hill-Robertson effect: evolutionary consequences of weak selection and linkage in finite populations. Heredity 100:19–31.

Corbett-Detig, R. B., J. Zhou, A. G. Clark, D. L. Hartl, and J. F. Ayroles. 2013. Genetic incompatibilities are widespread within species. Nature 504:135–7.

Crow, J. F. 1970. Genetic loads and the cost of natural selection. Pp. 128–177, in K.-i. Kojima, ed. Mathematical Topics in Population Genetics. Springer, Berlin.

Cutter, A. D. 2012. The polymorphic prelude to Bateson–Dobzhansky–Muller incompatibilities. Trends Ecol. Evol. 27:209–218.

Dobzhansky, T. 1937. Genetics and the Origin of Species. Columbia Univ. Press, New York, NY.

Felsenstein, J. 1974. The evolutionary advantage of recombination. Genetics 78:737–756.

Gaffney, D. J., and P. D. Keightley. 2006. Genomic selective constraints in murid noncoding DNA. PLoS Genet. 2:e204.

García-Ramos, G., and M. Kirkpatrick. 1997. Genetic models of adaptation and gene flow in peripheral populations. Evolution 51:21–28.

Gibson, A. K., L. F. Delph, and C. M. Lively. 2017. The two-fold cost of sex: Experimental evidence from a natural system. Evol. Lett. 1:6–15.

Gordo, I., and P. R. A. Campos. 2008. Sex and deleterious mutations. Genetics 179:621–626.

Haag-Liautard, C., M. Dorris, X. Maside, S. Macaskill, D. L. Halligan, B. Charlesworth, and P. D. Keightley. 2007. Direct estimation of per nucleotide and genomic deleterious mutation rates in *Drosophila*. Nature 445:82–85.

Haigh, J. 1978. The accumulation of deleterious genes in a population— Muller's ratchet. Theor. Popul. Biol. 14:251–267.

Hartfield, M., S. P. Otto, and P. D. Keightley. 2010. The role of advantageous mutations in enhancing the evolution of a recombination modifier. Genetics 184:1153–1164.

———. 2012. The maintenance of obligate sex in finite, structured populations subject to recurrent beneficial and deleterious mutation. Evolution 66:3658–3669.

Hendry, A. P., T. Day, and E. B. Taylor. 2001. Population mixing and the adaptive divergence of quantitative traits in discrete populations: a theoretical framework for empirical tests. Evolution 55:459–466.

Hill, W. G., and A. Robertson. 1966. The effect of linkage on limits to artificial selection. Genet. Res. 8:269–294.

Ihaka, R., and R. Gentleman. 1996. R: a language for data analysis and graphics. J. Comp. Graph. Stat. 5:299–314.

Iles, M. M., K. Walters, and C. Cannings. 2003. Recombination can evolve in large finite populations given selection on sufficient loci. Genetics 165:2249–2258.

Judson, O. P. 1997. A model of asexuality and clonal diversity: Cloning the Red Queen. J. Theor. Biol. 186:33–40.

Kalirad, A., and R. B. R. Azevedo. 2017. Spiraling Complexity: A Test of the Snowball Effect in a Computational Model of RNA Folding. Genetics 206:377–388.

Keightley, P. D., and S. P. Otto. 2006. Interference among deleterious mutations favours sex and recombination in finite populations. Nature 443:89–92.

Khatri, B. S., and R. A. Goldstein. 2015. Simple biophysical model predicts faster accumulation of hybrid incompatibilities in small populations under stabilizing selection. Genetics 201:1525–1537.

Kimura, M. 1952. "Stepping-stone" model of population. Natl. Inst. Genet. Jpn. 3:62–63.

Kirkpatrick, M., and N. H. Barton. 1997. Evolution of a species' range. Am. Nat. 150:1–23.

Kirkpatrick, M., and C. D. Jenkins. 1989. Genetic segregation and the maintenance of sexual reproduction. Nature 339:300–301.

Kondrashov, A. S., and J. F. Crow. 1991. Haploidy or diploidy: which is better? Nature 351:314–315.

Ladle, R. J., R. A. Johnstone, and O. P. Judson. 1993. Coevolutionary dynamics of sex in a metapopulation: escaping the Red Queen. Proc. R. Soc. B 253:155–160.

Lehtonen, J., M. D. Jennions, and H. Kokko. 2012. The many costs of sex. Trends Ecol. Evol. 27:172–178.

Lohaus, R., C. L. Burch, and R. B. R. Azevedo. 2010. Genetic architecture and the evolution of sex. J. Hered. 101:S142–S157.

MacCarthy, T., and A. Bergman. 2007. Coevolution of robustness, epistasis, and recombination favors asexual reproduction. Proc. Natl. Acad. Sci. USA 104:12801–12806.

Maheshwari, S., and D. A. Barbash. 2011. The genetics of hybrid incompatibilities. Annu. Rev. Genet. 45:331–355.

Martin, G., S. P. Otto, and T. Lenormand. 2006. Selection for recombination in structured populations. Genetics 172:593–609.

Martin, O. C., and A. Wagner. 2009. Effects of recombination on complex regulatory circuits. Genetics 183:673–684.

Maynard Smith, J. 1978. The evolution of sex. Cambridge Univ. Press, Cambridge, MA.

Muller, H. J. 1942. Isolating mechanisms, evolution and temperature. Biol. Symp. 6:71–125.

———. 1964. The relation of recombination to mutational advance. Mutat. Res. 1:2–9.

Nowak, S., J. Neidhart, I. G. Szendro, and J. Krug. 2014. Multidimensional epistasis and the transitory advantage of sex. PLoS Comput. Biol. 10:e1003836.

Otto, S. P. 2003. The advantages of segregation and the evolution of sex. Genetics 164:1099–1118.

Otto, S. P., and N. H. Barton. 2001. Selection for recombination in small populations. Evolution 55:1921–1931.

Otto, S. P., and T. Lenormand. 2002. Resolving the paradox of sex and recombination. Nat. Rev. Genet. 3:252–261.

Otto, S. P., and S. L. Nuismer. 2004. Species interactions and the evolution of sex. Science 304:1018–1020.

Palmer, M. E., and M. W. Feldman. 2009. Dynamics of hybrid incompatibility in gene networks in a constant environment. Evolution 63:418–431.

Peck, J. R., J. Yearsley, and G. Barreau. 1999. The maintenance of sexual reproduction in a structured population. Proc. R. Soc. B 266:1857–1863.

Poon, A., and S. P. Otto. 2000. Compensating for our load of mutations: Freezing the meltdown of small populations. Evolution 54:1467–1479.

Presgraves, D. C. 2010. The molecular evolutionary basis of species formation. Nat. Rev. Genet. 11:175–180.

Salathé, M., R. Salathé, P. Schmid-Hempel, and S. Bonhoeffer. 2006. Mutation accumulation in space and the maintenance of sexual reproduction. Ecol. Lett. 9:941–946.

Shields, W. M. 1982. Philopatry, Inbreeding, and the Evolution of Sex. State Univ. of New York Press, Albany, NY.

Siller, S. 2001. Sexual selection and the maintenance of sex. Nature 411:689–692.

Tulchinsky, A. Y., N. A. Johnson, W. B. Watt, and A. H. Porter. 2014. Hybrid incompatibility arises in a sequence-based bioenergetic model of transcription factor binding. Genetics 198:1155–1166.

Vrijenhoek, R. C. 1998. Animal clones and diversity. BioScience 48:617–628.

Wagner, A. 1994. Evolution of gene networks by gene duplications: A mathematical model and its implications on genome organization. Proc. Natl. Acad. Sci. USA 91:4387–4391.

———. 1996. Does evolutionary plasticity evolve? Evolution 50:1008–1023.

Weinreich, D. M., R. A. Watson, and L. Chao. 2005. Perspective: Sign epistasis and genetic constraint on evolutionary trajectories. Evolution 59:1165–1174.

Whitlock, A. O. B., K. M. Peck, R. B. R. Azevedo, and C. L. Burch. 2016. An evolving genetic architecture interacts with Hill–Robertson interference to determine the benefit of sex. Genetics 203:923–936.

Supporting Information

Additional supporting information may be found online in the Supporting Information section at the end of the article.

Figure S1. Changes in mean fitness ($\overline{W}$) over time in asexual (open circles) and sexual (filled circles) populations evolving under the migration rate (m) and deme size (N_d) indicated inside each panel.

Figure S2. Estimation of the maximum cost of sex at which sexual populations resist invasion by asexual mutants (maintenance-C_{max}).

Figure S3. Estimation of the maximum cost of sex at which sexual mutants successfully invade equilibrium asexual populations (origin-C_{max}).

Figure S4. The distributions of mutational and epistatic effects on fitness in the founding clones and in equilibrium evolved populations.

Figure S5. Evolution of the distribution of mutation effects.

Figure S6. Network connectivity (γ) has a quantitative effect on fitness and genetic architecture equilibria.

Figure S7. The genome wide mutation rate (U) has a quantitative effect on fitness and genetic architecture equilibria.